Letter

Machine learning study of highly spin-polarized Heusler alloys at finite temperature

Ivan Kurniawan [1,2] Yoshio Miura [1,3,*] and Kazuhiro Hono [1,2]

[1]*Research Center for Magnetic and Spintronics Materials, National Institute for Materials Science (NIMS), 1-2-1 Sengen, Tsukuba 305-0047, Japan*

[2]*Graduate School of Science and Technology, University of Tsukuba, Tsukuba 305-8577, Japan*

[3]*Center for Spintronics Research Network (CSRN), Graduate School of Engineering Science, Osaka University, Machikaneyama 1-3, Toyonaka, Osaka 560-8531, Japan*

(Received 10 June 2022; accepted 31 August 2022; published 14 September 2022)

A huge magnetoresistance (MR) ratio exceeding 2000% at cryogenic temperature that was reported for half-metallic Heusler alloy based magnetic tunnel junctions showed large degradation at room temperature, which impedes practical application of Heusler alloy based MR devices. This motivates us to explore alternative Heusler alloys that show high spin polarization at finite temperatures. Here, we propose half-metallic Heusler alloys based on finite-temperature first-principles calculation via the disordered local moment method together with machine learning. We found several prospective materials at room temperature such as $Co_2MnGa_{0.2}As_{0.8}$ and $Co_2FeAl_{0.4}Sn_{0.6}$. We also investigated two combinatorial series, $Co_2MnGa_yAs_{1-y}$ and $Co_2FeAl_ySn_{1-y}$, to understand the effect of alloy mixing on temperature dependence and found that Fermi level tuning significantly improved the spin polarization and its temperature dependence, especially in $Co_2FeAl_ySn_{1-y}$.

DOI: 10.1103/PhysRevMaterials.6.L091402

I. INTRODUCTION

Magnetoresistance (MR) in magnetic tunnel junctions (MTJs) is one of the most important phenomena for the realization of spintronics applications, such as magnetic random access memories [1] and magnetoresistive sensors [2]. Recently, high-throughput calculations have been widely performed to obtain novel magnetic materials with high spin polarization around Fermi level (so-called half-metals) [3–7], because the high spin polarization is crucial to obtaining sufficient magnetoresistance for the applications. In particular, Heusler alloys, a family of A_2BC compounds, have been actively explored by machine learning due to the abundant variety of atomic combinations and the relatively simple fabrication process. However, the machine learning investigation of highly spin-polarized Heusler alloys with first-principles calculations has been performed at zero temperature [7]. This made a significant discrepancy between physical properties designed by first-principles calculations and experimental results of the predicted material.

One of the most serious problems of half-metallic Heusler alloys in spintronic device application is the reduction of magnetoresistance at room temperature (the large temperature dependence) in tunnel magnetoresistance (TMR) and the current perpendicular to plane giant magnetoresistive (CPP-GMR) devices [8,9]. This means that simple ground-state calculations of spin polarization at 0 K are not enough to predict half-metallicity at ambient temperature. In our previous work, we performed finite-temperature calculations of half-metallic electronic structures of Co-based full Heusler alloys and found that the conduction bands of the Co d orbital significantly degrade the spin polarization at room temperature [10]. Experimentally, tuning the Fermi level via alloying of different elements, such as $Co_2Fe(Al_{0.5}Si_{0.5})$ [11], is also important to improve the large temperature dependence of spin polarizations. These previous experimental and theoretical studies suggest that for realization of spintronics applications, machine learning with finite-temperature first-principles calculations is necessary to predict novel half-metallic Heusler alloys at room temperature.

The purpose of the present work was to search for alternative half-metallic Heusler alloys having high spin polarization at room temperature using machine learning and the finite-temperature first-principles calculations. Due to the multielement character of Heusler alloys, machine learning is a suitable material informatics tool for multidimensional analysis. Recently, using a deep neural network, Hu *et al.* predicted >100 highly spin-polarized and six prospective half-metal from >10 000 Heusler A_2BC candidates at 0 K [7]. In contrast to the previous work, we incorporate the finite-temperature effect via the disordered local moment (DLM) method to clarify the spin polarization of ternary, quaternary, and quinary Heusler alloys at finite temperature [10,12]. We successfully predict alternative quaternary Heusler alloys on the basis of finite-temperature machine learning and first-principles calculations, such as $Co_2MnGa_{0.2}As_{0.8}$ and $Co_2FeAl_{0.4}Sn_{0.6}$, which show high spin polarization even at room temperature.

II. METHOD

We prepare a list of candidates of Heusler compounds with the general composition of $A_2(B_xB'_{1-x})(C_yC'_{1-y})$ (x and y are

*Corresponding author: miura.yoshio@nims.go.jp

coefficients from 0.0 to 1.0 with a 0.2 interval). Elements for A, B (B') and C (C') sites are taken from the distribution of components predicted by Hu *et al.* (A = Fe, Co, Ru, Rh; B, B' = Sc, Ti, V, Cr, Mn, Fe, Y, Zr, Nb, Mo; C, C' = Al, Si, P, Ga, Ge, As, In, Sn, Sb) [7]. These combinations lead to 73 440 different compositions. Each candidates assumes the $L2_1$ structure, which has four atoms located on interpenetrating fcc sublattices, consisting of two A atoms at (0.25, 0.25, 0.25) and (0.75, 0.75, 0.75), the B (B') atoms at (0.00, 0.00, 0.00), and the C (C') atoms at (0.50, 0.50, 0.50). The lattice constants of ternary alloys were taken from the Heusler Database of The University of Alabama [13] and the supplementary information from Hu *et al.* [7]. Using Vegard's law [14], the lattice constants of quaternary and quinary Heusler composition were extrapolated.

The computational procedures to calculate spin polarization at finite temperature are divided into two steps. First, spin-polarized electronic structure calculations at zero temperature were performed by multiple-scattering Green's function formalism in the Korringa-Kohn-Rostoker (KKR) method [15,16] implemented in the HUTSEPOT code [17]. Local spin density approximation (LSDA) by Perdew and Wang [18] was selected for the exchange-correlation functional and a $20\times20\times20$ k mesh was used. The core and valence electrons were treated within the scalar-relativistic approximation and the angular momentum expansion of scattering matrices in a basis of spherical harmonics is truncated at $l_{\max} = 3$. To deal with the atomic disorder, we used coherent potential approximation (CPA) [19]. The Kohn-Sham potential was determined using atomic-sphere approximation (ASA). Second, after obtaining the ground-state potential from the first step as the "frozen" potential, we introduced the finite-temperature effect using the DLM method [20]. This effect assumes that magnetic compounds consist of local moments that fluctuate at finite temperature and have a longer stabilization timescale than electron motion [20]. Therefore, the scalar-relativistic Kohn-Sham-Dirac equation was solved non-self-consistently within the ASA until it reached the convergence of the iterative temperature value with the starting parameter of the Weiss field as the "average mean field." Details of the technical description of the DLM approach are given elsewhere [10,12,20].

Total *spd* (total) spin polarization at zero and finite temperature is evaluated by

$$P_{spd} = \frac{D^{\uparrow}_{spd}(E_{\rm F}) - D^{\downarrow}_{spd}(E_{\rm F})}{D^{\uparrow}_{spd}(E_{\rm F}) + D^{\downarrow}_{spd}(E_{\rm F})}, \tag{1}$$

where $D^{\uparrow}_{spd}(E_{\rm F})$ and $D^{\downarrow}_{spd}(E_{\rm F})$ correspond to the total *spd* density of states (DOS) on the Fermi level of majority and minority spins, respectively. Despite the dependency of the MR ratio on many factors such interface quality, defect, vacancy, lattice mismatch, etc., we only focus on the reduced bulk *sp* spin polarization at finite temperature in this study. It has been demonstrated that *sp* spin polarization has good agreement with spin polarization extracted from the experimental TMR ratio using Julliere's model [21,22]. Furthermore, experimental studies of CPP-GMR suggested that CPP-GMR ratios are more properly explained by *sp* spin polarization due to the negligible contribution of localized character *d* electrons to the transport properties [23]. Therefore, we calculated *sp* spin polarization, which is defined as

$$P_{sp} = \frac{D^{\uparrow}_{sp}(E_{\rm F}) - D^{\downarrow}_{sp}(E_{\rm F})}{D^{\uparrow}_{sp}(E_{\rm F}) + D^{\downarrow}_{sp}(E_{\rm F})}, \tag{2}$$

where $D^{\uparrow}_{sp}(E_{\rm F})$ and $D^{\downarrow}_{sp}(E_{\rm F})$ correspond to the *sp* DOS on the Fermi level of majority and minority spin, respectively.

Our main purpose was to find an alternative Heusler alloy composition that retains the high spin polarization at finite temperature. Due to the complex relation between the output (high spin polarization) and the input (composition), this problem can be assumed as a black-box function, and Bayesian optimization is adopted to find its solution with high efficiency. In this work, the open-source PYTHON library called COMBO [24] was employed to perform the optimization process.

Aside from the optimization method, there are other three required components for the machine learning process: the descriptor, the evaluator, and the calculator [25]. We set the descriptor to identify each composition $A_2(B_xB'_{1-x})(C_yC'_{1-y})$ as a concatenation of integer numbers following the rule

$$\begin{aligned} A_2(B_xB'_{1-x})(C_xC'_{1-x}) \rightarrow {\rm P|G}_A + {\rm P|G}_B + n_x + {\rm P|G}_{B'} \\ + n_{1-x} + {\rm P|G}_C + n_y + {\rm P|G}_{C'} \end{aligned} \tag{3}$$

where P|G is a set of the number of period and group in the periodic table to identify the element (A, B, B', C, C') and n indicates the stoichiometry coefficient of B, B', C, and C'. For example, Co(Si) is in the fourth (third) period and ninth (14th) group; thus we express the ${\rm P|G}_{\rm Co} = 4|9 \Rightarrow 49$ (${\rm P|G}_{\rm Si} = 3/14 \Rightarrow 314$), respectively. The stoichiometry coefficient of n_x and n_y were described as follows, $x = 0.2 \Rightarrow n_x = 02$, and $y = 1.0 \Rightarrow n_y = 10$, and so on. If there is no $B'(C')$ element, we set ${\rm P|G}_{B'} \Rightarrow 00$ (${\rm P|G}_{C'} \Rightarrow 00$) and $n_{1-x} = 00$ ($n_{1-y} = 00$), respectively. By concatenating all of these parameters, each composition will be uniquely described with a 20-digit integer descriptor. For example, the Heusler alloy $Ru_2(Mn_{0.6}Fe_{0.4})(P_{0.2}Sb_{0.8})$ can be expressed by "58 47 06 48 04 315 02 515 08" due to ${\rm P|G}_{\rm Ru} = 58$, ${\rm P|G}_{\rm Mn} = 47$, $n_x = 06$, ${\rm P|G}_{\rm Fe} = 48$, $n_{1-x} = 04$, ${\rm P|G}_{\rm P} = 315$, $n_y = 02$, ${\rm P|G}_{\rm Sb} = 515$, and $n_{1-y} = 08$.

The framework of the *ab initio* calculations and Materials Informatics (MI) procedures is illustrated in Fig. 1. First, we define the set of candidates [see Fig. 1(a)], and the first 20 compositions were chosen randomly to train the Bayesian regression as the machine learning model [see Fig. 1(b)]. The performance of each candidate was evaluated with the score defined by

$$\text{score} = T_{\rm conv} P_{sp}(T_{\rm conv}). \tag{4}$$

The $T_{\rm conv}$ and $P_{sp}(T_{\rm conv})$ were the converged temperature and the *sp* spin polarization at $T_{\rm conv}$, which were obtained based on the DLM calculations at finite temperature [see Fig. 1(c)]. We adopted the spin polarization of *sp* states P_{sp} at finite temperature as the evaluator (score) of the Bayesian optimization, because the P_{sp} is more suitable than the P_{spd} (total spin polarization) to describe the spin-dependent transport in TMR and CPP-GMR devices.

The obtained score is used to estimate the black-box function which is expensive to calculate. This estimation model

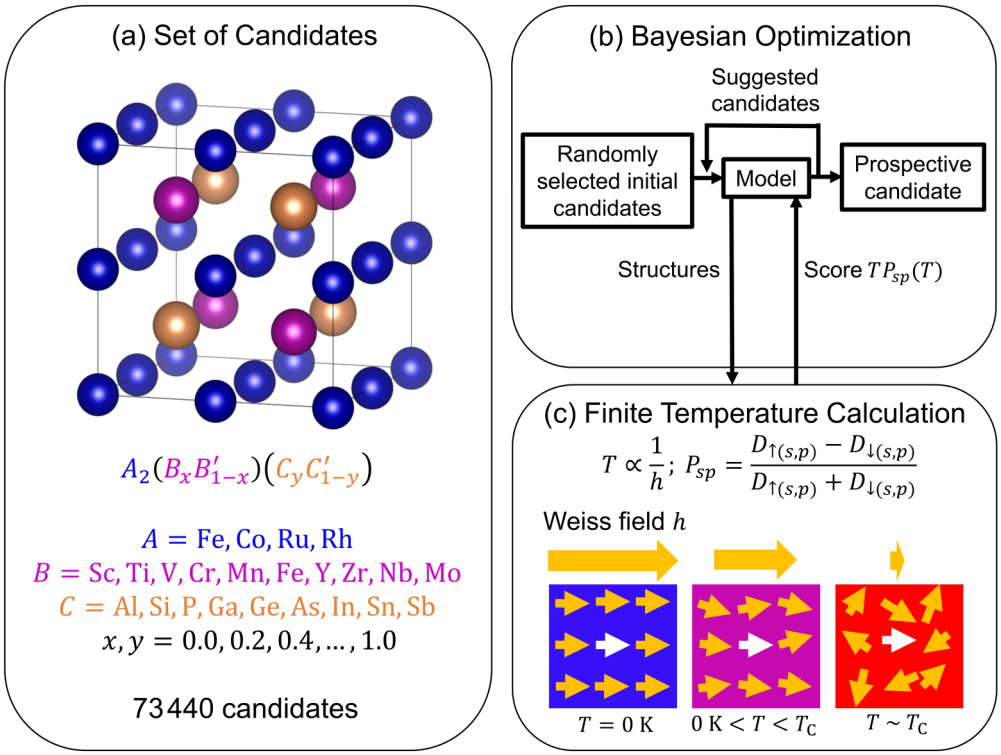

FIG. 1. The schematic workflow for finding prospective candidates with highly spin-polarized Heusler alloys at finite temperature. (a) Set of candidates to be investigated in this study, (b) implemented Bayesian optimization procedure to find the prospective candidate, and (c) finite-temperature calculation to obtain the *sp* spin polarization at converged temperature T using starting parameter of Weiss field h.

based on the Bayesian statistics will predict the next candidate that needs to be evaluated. First, we randomly selected 20 structures with respective descriptors for initial calculations. The scores of these 20 structures are evaluated via first-principles calculation, and used to train the Bayesian regression model. Then, in every round the next ten candidates are chosen by this estimation model and the corresponding scores of these ten candidates are added, repetitively, to improve the estimation model, until a fixed number of 2200 candidates (220 rounds) are evaluated. In this study, the best candidates are chosen according to the Thompson sampling criterion. Since Bayesian optimization is a widely used machine learning framework, details are written elsewhere [24].

III. RESULTS AND DISCUSSIONS

In Fig. 2, we show the score of the Bayesian optimization as a function of the number of calculated structures for the P_{sp} of Heusler alloys, indicating the performance of Bayesian optimization. As shown in Fig. 2, after several iteration processes, Bayesian optimization converges to the best candidates with the largest score, which corresponds to the Heusler alloy compositions that retain high spin polarization at finite temperature.

In Table I, we show the top 30 compounds having high scores in the Bayesian optimization together with the lattice constant a, the spin moment m_{total}, total and *sp* spin polarizations P_{spd} and P_{sp} at the converged temperature T_{conv}, and also the formation energy E_{form}, which are outputs of the first-principles calculations except for the lattice constants. Scores of $(P_{sp}T_{\text{conv}})$ are used in predictions of black-box function in Bayesian optimization. The formation energy E_{form} of $A_2(B_xB'_{1-x})(C_yC'_{1-y})$ was calculated by the following equation,

$$E_{\text{form}} = E^{\text{total}}_{A_2(B_xB'_{1-x})(C_yC'_{1-y})} - \left[2E^{\text{total}}_{A} + xE^{\text{total}}_{B} + (1-x)E^{\text{total}}_{B'} + yE^{\text{total}}_{C} + (1-y)E^{\text{total}}_{C'}\right] \quad (5)$$

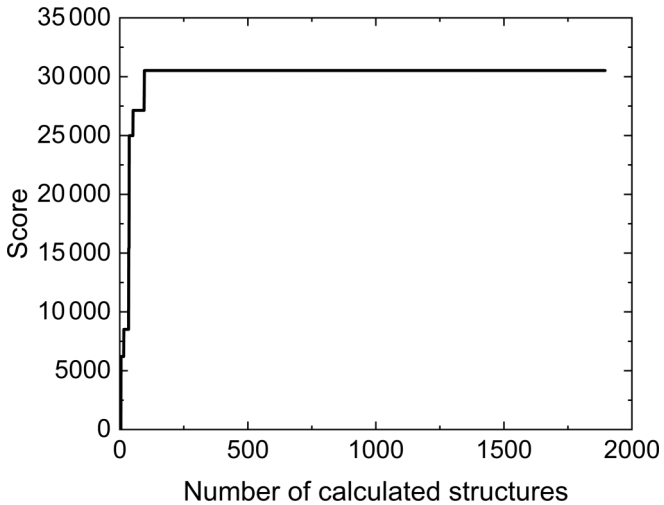

FIG. 2. Bayesian optimization performance for the calculated Heusler structures.

TABLE I. Summary of potential highly spin-polarized Heusler alloys at finite temperature suggested by Bayesian optimization.

System	a (Å)	m_{total} (μ_B)	T_{conv} (K)	P_{spd} (%)	P_{sp}(%)	$T_{\text{conv}}P_{sp}$	E_{form}(eV/f.u.)
$Co_2Fe_{1.0}Al_{1.0}$	5.700	4.86	352	39.0	86.7	30521	–1.71
$Co_2Fe_{1.0}Ga_{1.0}$	5.720	4.94	329	25.1	82.4	27134	–3.11
$Co_2Fe_{1.0}In_{1.0}$	5.980	5.10	305	11.4	79.8	24347	–3.38
$Co_2Mn_{1.0}As_{1.0}$	5.796	5.96	278	46.0	70.8	19684	–0.71
$Co_2Mn_{1.0}P_{1.0}$	5.638	5.67	223	4.6	77.1	17230	–1.79
$Co_2Mn_{1.0}Si_{1.0}$	5.630	5.00	299	79.0	88.0	26326	–2.44
$Co_2Fe_{1.0}Al_{0.4}Sn_{0.6}$	5.876	5.29	334	–1.7	85.0	28419	–3.09
$Co_2Fe_{1.0}Ga_{0.2}Ge_{0.8}$	5.736	5.32	280	–23.7	76.9	21485	–1.61
$Co_2Fe_{1.0}Ga_{0.2}In_{0.8}$	5.928	5.06	310	15.3	80.4	24920	–3.18
$Co_2Fe_{1.0}Ga_{0.4}Ge_{0.6}$	5.732	5.26	322	–7.4	82.4	26502	–2.00
$Co_2Fe_{1.0}Ga_{0.4}In_{0.6}$	5.876	5.03	315	18.7	80.9	25476	–3.04
$Co_2Fe_{1.0}In_{0.4}Sn_{0.6}$	5.988	5.40	324	–2.5	83.3	27009	–4.00
$Co_2Mn_{1.0}Al_{0.2}As_{0.8}$	5.777	5.61	300	66.8	89.0	26681	–0.97
$Co_2Mn_{1.0}Al_{0.2}Ge_{0.8}$	5.728	4.80	212	74.8	83.1	17589	–1.48
$Co_2Mn_{1.0}Al_{0.2}Sb_{0.8}$	5.954	5.55	276	60.5	87.8	24250	–0.26
$Co_2Mn_{1.0}Al_{0.2}Si_{0.8}$	5.644	4.80	237	80.5	88.2	20909	–2.29
$Co_2Mn_{1.0}Ga_{0.2}As_{0.8}$	5.781	5.61	291	65.1	88.4	25711	–1.23
$Co_2Mn_{1.0}Ga_{0.2}Ge_{0.8}$	5.731	4.81	208	73.3	82.2	17088	–1.75
$Co_2Mn_{1.0}Ga_{0.2}Sb_{0.8}$	5.958	5.56	268	58.2	86.8	23254	–0.45
$Co_2Mn_{1.0}Ga_{0.4}As_{0.6}$	5.765	5.20	264	71.2	86.4	22836	–1.73
$Co_2Mn_{1.0}Ga_{0.4}Sb_{0.6}$	5.898	5.21	246	67.6	83.6	20525	–0.89
$Co_2Ti_{0.2}Mn_{0.8}Ge_{1.0}$	5.756	4.39	216	66.7	88.0	18998	–1.62
$Co_2Fe_{0.8}Mo_{0.2}As_{0.2}Sb_{0.8}$	5.979	4.60	267	37.4	81.1	21680	0.60
$Co_2Fe_{0.8}Mo_{0.2}In_{0.2}Sb_{0.8}$	6.037	4.80	264	44.9	82.4	21737	–0.13
$Co_2Fe_{0.8}Mo_{0.2}Sn_{0.4}Sb_{0.6}$	6.039	4.78	265	47.0	83.2	22002	–1.27
$Co_2Fe_{0.8}Nb_{0.2}In_{0.6}Sb_{0.4}$	6.032	4.81	244	31.2	80.6	19692	–1.70
$Co_2Mn_{0.8}Fe_{0.2}Ge_{0.4}Sb_{0.6}$	5.902	5.51	230	–7.0	75.4	17302	–0.20
$Co_2Mn_{0.8}Fe_{0.2}In_{0.4}Sb_{0.6}$	6.001	5.40	270	54.4	83.5	22585	–1.40
$Co_2Mn_{0.8}Fe_{0.2}Sn_{0.6}Sb_{0.4}$	6.000	5.54	275	45.9	86.3	23748	–2.79
$Co_2Mn_{0.8}Nb_{0.2}Ge_{0.2}As_{0.8}$	5.773	4.90	226	74.9	89.0	20158	–0.63
$Co_2Mn_{0.8}Nb_{0.2}Ge_{0.4}As_{0.6}$	5.763	4.78	207	76.8	88.0	18251	–0.77
$Co_2Mn_{0.8}Zr_{0.2}P_{0.2}Ge_{0.8}$	5.760	4.50	203	37.8	83.1	16836	–1.22

where E^{total} is the total energy for each system for Heusler alloys $A_2(B_xB'_{1-x})(C_yC'_{1-y})$, and single elements A, B, B', C, and C' are calculated using first-principles calculation at zero temperature.

As shown in Table I, despite considering many elements in the A and B sites, the majority of prospective candidates have Co occupy the A site, to be specific, Co_2Fe- and Co_2Mn-based Heusler alloys which consist of three-, four-, and five-element compounds. The magnetic moments of these candidates are pretty high, more than 4.5 μ_B, which leads to converged temperature around 200–350 K using the same starting parameter Weiss field. Interestingly, these candidates have various value of P_{spd} spanned over the range –20%–80%, despite the relatively high P_{sp} being more than 70%. This result implies a conventional approach to find the highly spin-polarized material based on merely P_{spd} value excluding many prospective candidates. Note that we also found that almost all potential candidates except $Co_2Fe_{0.8}Mo_{0.2}As_{0.2}Sb_{0.8}$ have negative formation energy, which confirms the thermodynamical stability of most of the proposed compounds.

In order to understand why the most prospective highly spin-polarized Heusler alloys suggested by Bayesian optimization are Co-based materials, we also evaluated the ground-state properties of all candidates by high-throughput calculations. Note that despite calculations of all candidates (73440 candidates in the system) were conducted, only 41612 calculations (∼56%) converged and obtained the solution. In Figs. 3(a)–3(c), we show the distributions of the converged calculation results for ground-state P_{spd} and P_{sp} values mapped on a two-dimensional plane over the A elements, the number of elements, and spin moments at 0 K, respectively. The conventional approach of finding highly spin-polarized material was done by "vertically scanning" over the candidates in the high-P_{spd} area (specified by sky blue rectangles). However, as mentioned previously, P_{sp} is more suitable to explain the magnetoresistance effect, so here we propose "horizontally scanning" over the high-P_{sp} area (specified by red rectangles). Based on Fig. 3(a), it is clear that the high-P_{sp} area is filled by the Co-based Heusler alloy. These candidates mainly consist of quaternary and quinary compounds as a consequence of the increase of the number of combinations with increasing the number of elements [see Fig. 3(b)]. It turned out that significant portions of these candidates also exhibit a large spin moment (4–6 μ_B) at 0 K [see Fig. 3(c)] which may imply high Curie temperature and therefore the

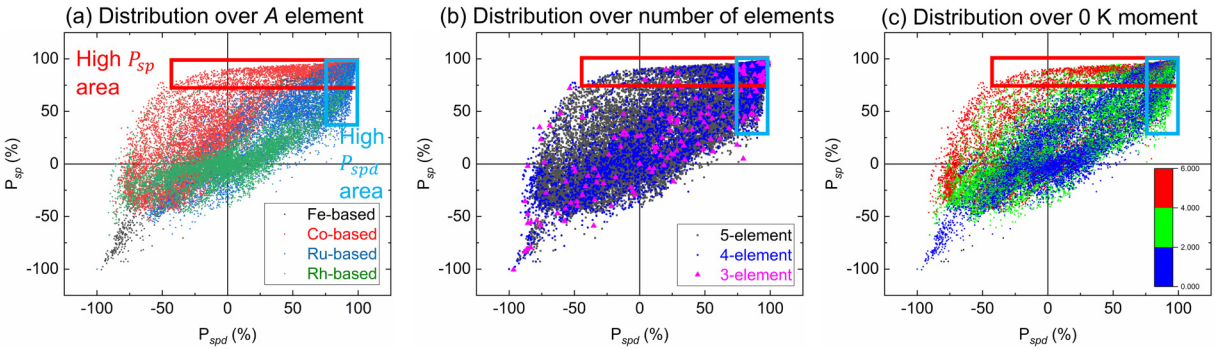

FIG. 3. The results of high-throughput calculation for ground-state properties of all candidates as (a) distribution over *A* element, (b) distribution over number of elements, and (c) distribution over 0 K moment.

robustness of spin polarization of Co-based Heusler alloys at finite temperature [26].

In order to understand the importance of including the finite-temperature effect, we picked some ternary compounds with relatively large magnetic moments (3–6 μ_B) and demonstrated $P_{sp} > 70\%$ at 0 K and plotted the P_{sp} at finite temperature in Fig. 4. We show P_{sp} of Co_2CrAl (3.00 μ_B), Fe_2MnP (4.00 μ_B), and Ru_2MnSb (4.00 μ_B) as representative cases of the large temperature dependence of P_{sp}. These materials show P_{sp} larger than 70% and almost half-metallic electronic structures at 0 K. However, P_{sp} of these compounds around 300 K is smaller than 50%. On the other hand, Co_2MnAs (5.98 μ_B) and Co_2FeIn (5.09 μ_B) show slow decay of P_{sp} with increasing temperature, preserving high spin polarization over 70% around 300 K. These results indicate that the inclusion of the finite-temperature effect in the first-principles calculations is necessary to find prospective Heusler alloys with machine learning. Note that in Fig. 4, one may find spin polarization for Co_2CrAl and Ru_2MnSb practically reduced to zero at the corresponding calculated Curie temperature. Due to the mean-field approximation, it is clear that the calculated Curie temperature is overestimated. However, we confirm that for the

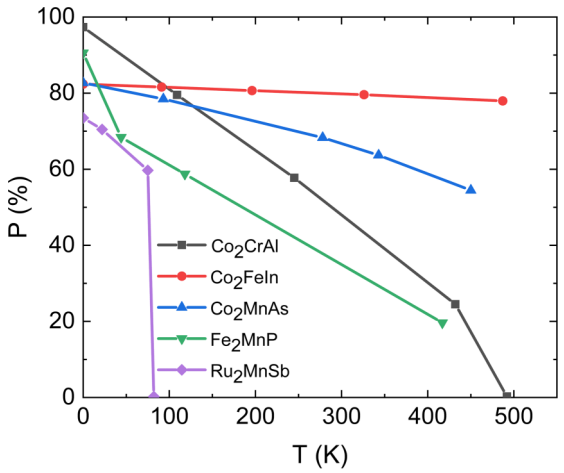

FIG. 4. The temperature dependence of P_{sp} of some ternary Heusler alloys that demonstrated large magnetic moment (3−6 μ_B) and spin polarization >70% at 0 K.

Co-based Heusler alloys, calculated Curie temperature is proportional with both experimental Curie temperature and magnetic moment (not shown here); therefore this DLM method is still adequate to discuss the finite-temperature properties.

Then we systematically investigated the combinatorial system for four prospective candidates ($Co_2MnGa_{0.2}As_{0.8}$, Co_2MnAs, $Co_2FeAl_{0.4}Sn_{0.6}$, and Co_2FeAl) to understand the relation between electronic structure and temperature dependence of spin polarization. In Figs. 5(a)–5(f), we show the temperature dependence of P_{spd} and P_{sp} of $Co_2MnGa_yAs_{1-y}$, and the density of states (DOS) for total and *sp* states, and P_{spd} and P_{sp} around the Fermi level.

Recently, Co_2MnGa was reported to show giant anomalous Nernst effect in the $L2_1$ structure [27]. Meanwhile, theoretical calculations of Co_2MnAs suggest a very large magnetic moment of 6 μ_B [28]. However, both of these compounds and their combinatorial alloy are not widely explored in terms of spin polarization and its application in magnetoresistance. Thus, $Co_2MnGa_{0.2}As_{0.8}$ (and $Co_2FeAl_{0.4}Sn_{0.6}$) obtained in this study by the Bayesian optimization with finite-temperature calculations are materials having high P_{sp} around room temperature. As shown in Fig. 5(a), despite the pretty high value of P_{spd} of Co_2MnAs at 0 K, Ga doping improves it further. This can be explained by considering the Fermi level tuning from Co_2MnAs (near the conduction band edge) to the Co_2MnGa (near the valence band edge) [see Figs. 5(b) and 5(c)]. Similarly, the effect of Ga doping is also observed in P_{sp} [see Figs. 5(d)–5(f)], which suggests $Co_2MnGa_{0.2}As_{0.8}$ and $Co_2MnGa_{0.4}As_{0.6}$ have superior spin polarization among the series. Note that despite the significant shift of the Fermi level for y from 0.0 to 0.8 for $Co_2MnGa_yAs_{1-y}$, the temperature dependence of P_{sp} does not change depending on y. This is because significant increase of minority spin states happens at the conduction band rather than the valence band edge. For $y = 0.0$, the Fermi level is already quite distant from the conduction band edge, therefore shifting further from the conduction band edge as increasing y does not affect the temperature dependence that much. This phenomenon is also observed experimentally in $Co_2MnAl_ySi_{1-y}$ with $y < 0.4$ by Sakuraba *et al.* [29].

Figure 6(a) shows the temperature dependence of P_{spd} for $Co_2FeAl_ySn_{1-y}$, (b) *spd* electronic structure at 0 K, (c) energy dependence of P_{spd} calculated at 0 K, and (d–(f) its

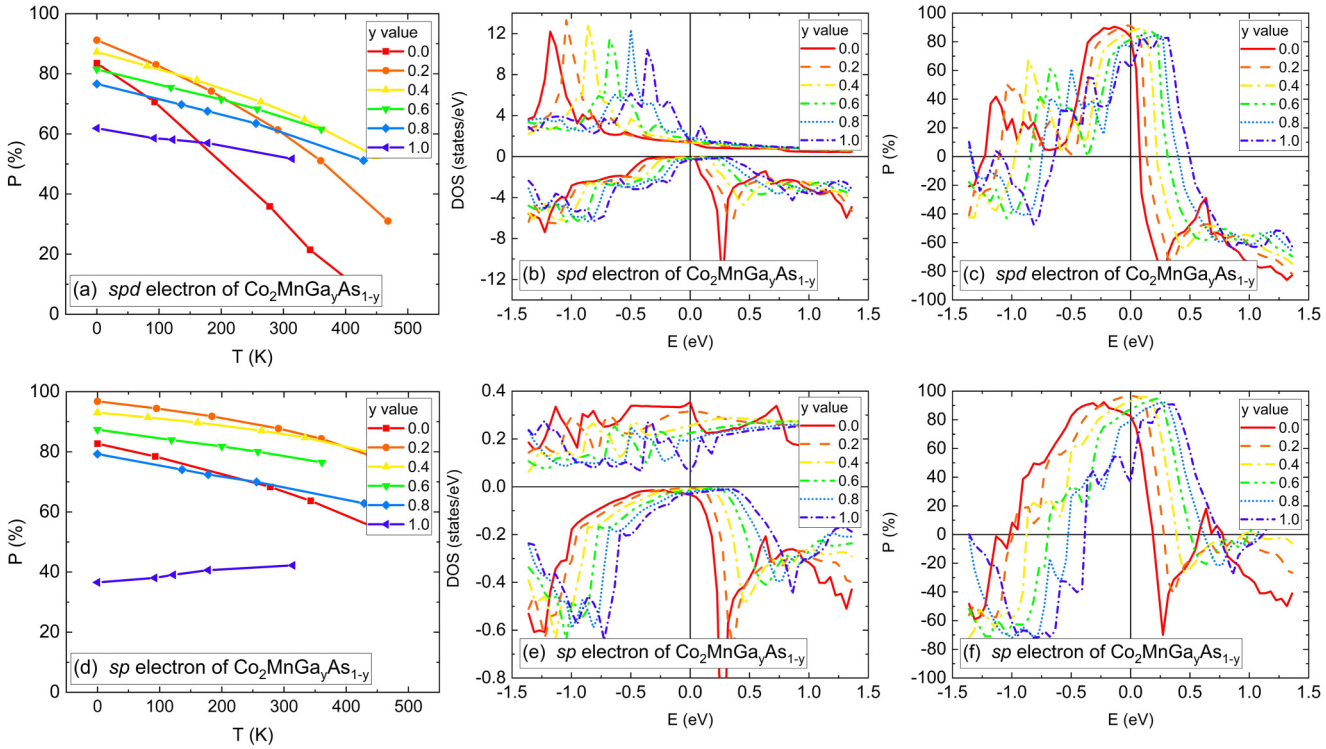

FIG. 5. (a) The temperature dependence of P_{spd} on value of y from $Co_2MnGa_yAs_{1-y}$, (b) *spd* electronic structure at 0 K, (c) energy dependence of P_{spd} calculated at 0 K, and (d)–(f) its counterpart for P_{sp} and *sp* electronic structure. The reference of the energy E is the Fermi energy.

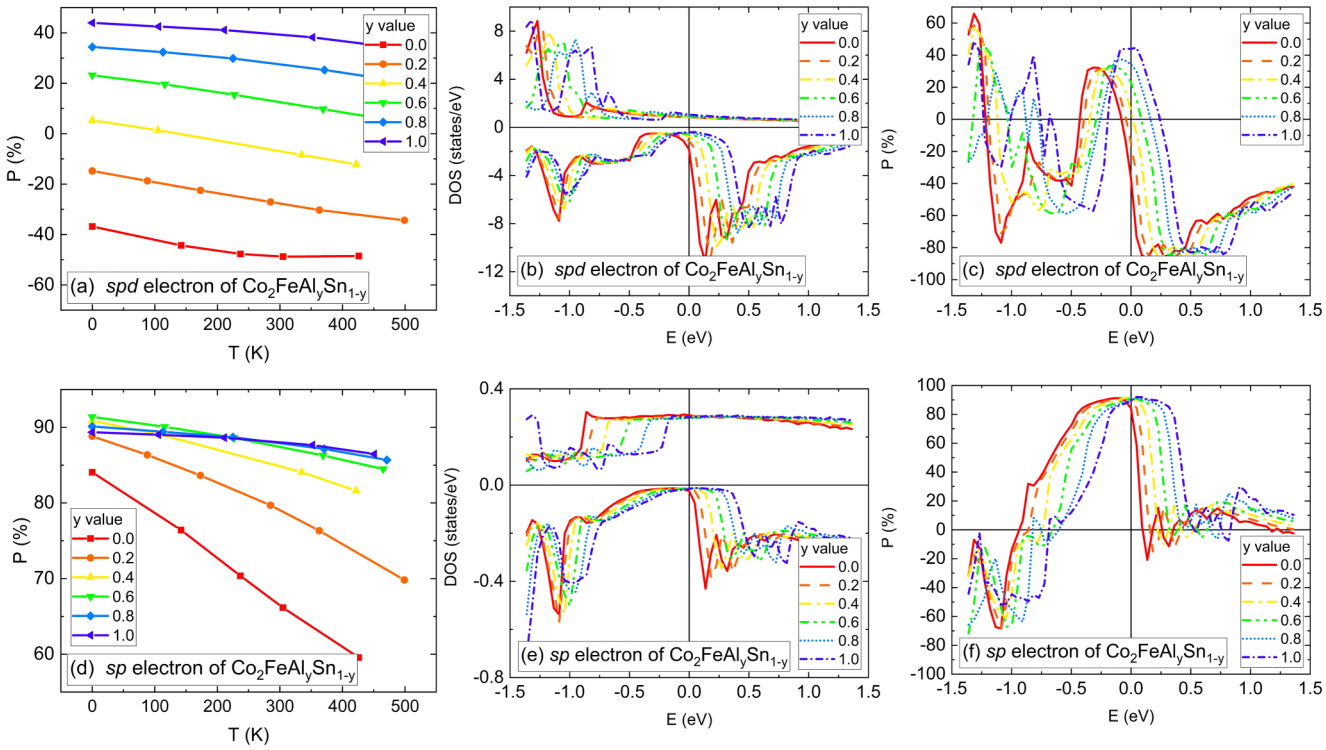

FIG. 6. (a) The temperature dependence of P_{spd} for $Co_2FeAl_ySn_{1-y}$, (b) *spd* electronic structure at 0 K, (c) energy dependence of P_{spd} calculated at 0 K, and (d)–(f) its counterpart for P_{sp} and *sp* electronic structure. The reference of the energy E is the Fermi energy.

counterpart for P_{sp} and sp electronic structure. As shown in Figs. 6(a)–6(c), the P_{spd} value and spd electronic structure of Co_2FeAl over a significant temperature range fail to explain the giant tunneling magnetoresistance (TMR) demonstrated especially in the Co_2FeAl/MgO-based MTJ [30]. It was widely understood that giant TMR effect in Fe/MgO-based MTJ is due to the spin-filtering effect of single-crystalline MgO in which Δ_1 symmetry Bloch states at the in-plane k-vector $\vec{k}_{||} = (0, 0)$ mainly propagate for one spin channel only because of the half-metallic character of the Δ_1 band in bcc Fe [31]. Due to the fact that s, p_z, d_{z^2} atomic orbitals are compatible with the Δ_1 symmetry, here we can roughly approximate the strength of the spin-filtering effect as spin polarization considering the sp electron. That explains why the TMR effect could be properly described by P_{sp} behavior instead of the very low value of P_{spd} [see Figs. 6(a) and 6(d)] which is consistent with the previous studies on Heusler alloy/MgO-based MTJ [21,22]. Our calculation shows that P_{sp} exhibits very low temperature dependence but still retains a high value of spin polarization for Co_2FeAl which also is consistent with estimated spin polarization from Julliere's model of TMR effect of Cr/Co_2FeAl/MgO/CoFe MTJ [32]. The sp electronic structure and energy dependence of spin polarization at 0 K shown in Figs. 6(e) and 6(f) indicated that shifting the Fermi level further enough from the conduction band edge will lead to lower temperature dependence. Mixing the Al with Sn will shift the Fermi level position toward the conduction band edge, resulting in lower spin polarization and stronger temperature dependence for high Sn-content composition. However, for $0.4 \leqslant y \leqslant 1.0$, the high spin polarization and small temperature dependence is still retained.

In summary, we successfully performed Bayesian optimization combined with finite-temperature calculation to find the highly spin-polarized Heusler alloys around room temperature. We found $Co_2MnGa_{0.2}As_{0.8}$ and $Co_2FeAl_ySn_{1-y}$ ($0.4 \leqslant y \leqslant 1.0$) can show high sp spin polarization at around 300 K. Our study emphasized the importance of P_{sp} instead of the P_{spd} value to explain the magnetoresistance effect, and the alloy mixing to find the more prospective candidate with a four- or five-element based compound. However, most sare Co-based Heusler alloys, which is supported by the results from high-throughput screening. We also investigated two combinatorial series, $Co_2MnGa_yAs_{1-y}$ and $Co_2FeAl_ySn_{1-y}$, to understand the effect of alloy mixing on the temperature dependence and superiority of $Co_2MnGa_{0.2}As_{0.8}$ and $Co_2FeAl_ySn_{1-y}$ ($0.4 \leqslant y \leqslant 1.0$) compared to other Co-based Heusler alloys. $Co_2FeAl_ySn_{1-y}$ has good lattice matching with fcc Ag and is promising as a ferromagnetic electrode for CPP-GMR with Ag spacer. Furthermore, $Co_2MnGa_yAs_{1-y}$ is expected to be an effective spin injection source into GaAs semiconductors because it is insensitive to diffusion of Ga and As. These results confirmed the importance of distancing the Fermi level position from the conduction band edge via alloy mixing to improve the temperature dependence of spin polarization.

ACKNOWLEDGMENTS

We are grateful to S. Mitani, Y. Sakuraba, T. Tadano, and K. Masuda of NIMS for valuable discussions on this work. We thank J. B. Staunton at the University of Warwick and C. E. Patrick at the University of Oxford for support on the DLM method. I.K. acknowledges NIMS for the provision of a NIMS junior research assistantship. This work was partly supported by Grants-in-Aid for Scientific Research (Grants No. 17H06152, No. 20H02190, and No. 22H04966) from the Japan Society for the Promotion of Science, Center for Spintronics Research Network (CSRN) of Osaka University, the Cooperative Research Project Program of the Research Institute of Electrical Communication in Tohoku University, and the Japan Science and Technology Agency (JST) CREST (Grant No. JPMJCR21O1). The computations were performed on a Numerical Materials Simulator at NIMS.

[1] S. Bhatti, R. Sbiaa, A. Hirohata, H. Ohno, S. Fukami, and S. N. Piramanayagam, Mater. Today **20**, 530 (2017).
[2] K. Fujiwara, M. Oogane, A. Kanno, M. Imada, J. Jono, T. Terauchi, T. Okuno, Y. Aritomi, M. Morikawa, M. Tsuchida, N. Nakasato, and Y. Ando, Appl. Phys. Express **11**, 023001 (2018).
[3] J. Ma, V. I. Hegde, K. Munira, Y. Xie, S. Keshavarz, D. T. Mildebrath, C. Wolverton, A. W. Ghosh, and W. H. Butler, Phys. Rev. B **95**, 024411 (2017).
[4] J. Ma, J. He, D. Mazumdar, K. Munira, S. Keshavarz, T. Lovorn, C. Wolverton, A. W. Ghosh, and W. H. Butler, Phys. Rev. B **98**, 094410 (2018).
[5] S. Sanvito, C. Oses, J. Xue, A. Tiwari, M. Zic, T. Archer, P. Tozman, M. Venkatesan, M. Coey, and S. Curtarolo, Sci. Adv. **3**, e160224 (2017).
[6] S. V. Faleev, Y. Ferrante, J. Jeong, M. G. Samant, B. Jones, and S. S. P. Parkin, Phys. Rev. Mater. **1**, 024402 (2017).
[7] X. Hu, Y. Zhang, S. Fan, X. Li, Z. Zhao, C. He, Y. Zhao, Y. Liu, and W. Xie, J. Phys.: Condens. Matter **32**, 205901 (2020).
[8] B. Hu, K. Moges, Y. Honda, H. X. Liu, T. Uemura, M. Yamamoto, J. I. Inoue, and M. Shirai, Phys. Rev. B **94**, 094428 (2016).
[9] J. W. Jung, Y. Sakuraba, T. T. Sasaki, Y. Miura, and K. Hono, Appl. Phys. Lett. **108**, 102408 (2016).
[10] K. Nawa, I. Kurniawan, K. Masuda, Y. Miura, C. E. Patrick, and J. B. Staunton, Phys. Rev. B **102**, 054424 (2020).
[11] R. Shan, H. Sukegawa, W. H. Wang, M. Kodzuka, T. Furubayashi, T. Ohkubo, S. Mitani, K. Inomata, and K. Hono, Phys. Rev. Lett. **102**, 246601 (2009).
[12] I. Kurniawan, K. Nawa, K. Masuda, Y. Miura, and K. Hono, Acta Mater. **218**, 117218 (2021).
[13] See http://heusleralloys.mint.ua.edu/ for University of Alabama MINT Heusler Database, 2015.
[14] A. R. Denton and N. W. Ashcroft, Phys. Rev. A **43**, 3161 (1991).
[15] J. Korringa, Physica **13**, 392 (1947).
[16] W. Kohn and N. Rostoker, Phys. Rev. **94**, 1111 (1954).

[17] M. Däne, M. Lüders, A. Ernst, D. Ködderitzsch, W. M. Temmerman, Z. Szotek, and W. Hergert, J. Phys.: Condens. Matter **21**, 045604 (2009).
[18] J. P. Perdew and Y. Wang, Phys. Rev. B **45**, 13244 (1992).
[19] P. Soven, Phys. Rev. **156**, 809 (1967).
[20] B. L. Gyorffy, A. J. Pindor, J. Staunton, G. M. Stocks, and H. Winter, J. Phys. F: Met. Phys. **15**, 1337 (1985).
[21] G. F. Li, Y. Honda, H. X. Liu, K. I. Matsuda, M. Arita, T. Uemura, M. Yamamoto, Y. Miura, M. Shirai, T. Saito, F. Shi, and P. M. Voyles, Phys. Rev. B **89**, 014428 (2014).
[22] K. Moges, Y. Honda, H. X. Liu, T. Uemura, M. Yamamoto, Y. Miura, and M. Shirai, Phys. Rev. B **93**, 134403 (2016).
[23] S. Li, T. Nakatani, K. Masuda, Y. Sakuraba, X. D. Xu, T. T. Sasaki, H. Tajiri, Y. Miura, T. Furubayashi, and K. Hono, Acta Mater. **142**, 49 (2018).
[24] T. Ueno, T. D. Rhone, Z. Hou, T. Mizoguchi, and K. Tsuda, Mater. Discov. **4**, 18 (2016).
[25] S. Ju, T. Shiga, L. Feng, Z. Hou, K. Tsuda, and J. Shiomi, Phys. Rev. X **7**, 021024 (2017).
[26] S. Wurmehl, G. H. Fecher, H. C. Kandpal, V. Ksenofontov, C. Felser, H. J. Lin, and J. Morais, Phys. Rev. B **72**, 184434 (2005).
[27] A. Sakai, Y. P. Mizuta, A. A. Nugroho, R. Sihombing, T. Koretsune, M. T. Suzuki, N. Takemori, R. Ishii, D. Nishio-Hamane, R. Arita, P. Goswami, and S. Nakatsuji, Nat. Phys. **14**, 1119 (2018).
[28] A. Bakhshayeshi, M. M. Sarmazdeh, R. T. Mendi, and A. Boochani, J. Electron. Mater. **46**, 2196 (2017).
[29] Y. Sakuraba, K. Takanashi, Y. Kota, T. Kubota, M. Oogane, A. Sakuma, and Y. Ando, Phys. Rev. B **81**, 144422 (2010).
[30] W. Wang, H. Sukegawa, R. Shan, S. Mitani, and K. Inomata, Appl. Phys. Lett. **95**, 182502 (2009).
[31] W. H. Butler, X. G. Zhang, T. C. Schulthess, and J. M. MacLaren, Phys. Rev. B **63**, 054416 (2001).
[32] W. Wang, H. Sukegawa, and K. Inomata, Phys. Rev. B **82**, 092402 (2010).